

# **Structural Optimization of Novel One-Dimensional Composite Based on In-situ Grown 1D CNTs with Amorphous Structure and 2D MoS<sub>2</sub> Nanosheets for Improved Li Storage**

Zhiming Cheng<sup>1</sup>, Zunxian Yang<sup>\*,1,2</sup>, Yuliang Ye<sup>1</sup>, Songwei Ye<sup>1</sup>, Hongyi Hong<sup>1</sup>, Zhiwei Zeng<sup>1</sup>, Zongyi Meng<sup>1</sup>, Qianting Lan<sup>1</sup>, Hui Zhang<sup>1</sup>, Ye Chen<sup>1</sup>, Jiaxiang Wang<sup>1</sup>, Yuting Bai<sup>1</sup>, Xudong Jiang<sup>1</sup>, Benfang Liu<sup>1</sup>, Jiajie Hong<sup>1</sup>, Tailiang Guo<sup>1,2</sup>, Zhenzhen Weng<sup>3</sup>, Yongyi Chen<sup>3</sup>

<sup>1</sup>National & Local United Engineering Research Center of Flat Panel Display Technology, Fuzhou University, Fuzhou 350108, P. R. China.

<sup>2</sup>Mindu Innovation Laboratory, Fujian Science & Technology Innovation Laboratory For Optoelectronic Information of China, Fuzhou, 350108, P.R. China

<sup>3</sup>Department of Physics, School of Physics and Information Engineering, Fuzhou University

## **Supporting Information**

---

\* Corresponding author should be addressed. Tel.: +86 591 8789 3299; Fax: +86 591 8789 2643  
E-mail: yangzunxian@hotmail.com (Z. Yang)

## Captions

**Table S1** Specific surface area of MoS<sub>2</sub>@C-L and MoS<sub>2</sub>@C-H.

**Table S2** EIS Fitting resistance of MoS<sub>2</sub>@C , MoS<sub>2</sub>@C-L and MoS<sub>2</sub>@C-H.

**Fig.S1** SEM images of **(a,e)** MoS<sub>2</sub>@C-L,**(b,e)** MoS<sub>2</sub>@C,**(c,e)** MoS<sub>2</sub>@C-H.

**Fig.S2** EDS mapping of MoS<sub>2</sub>@C **(b)** C, **(c)** Mo, **(c)** S.

**Fig.S3** SEM images of **(a)** MoS<sub>2</sub>@C-L,**(b)** MoS<sub>2</sub>@C-L2,**(c)** MoS<sub>2</sub>@C-L4, **(d)**MoS<sub>2</sub>@C-L8, **(e)**MoS<sub>2</sub>@C-L12, **(f)** MoS<sub>2</sub>@C-L.

**Fig.S4** SEM images of **(a)** MoS<sub>2</sub>@C-H1, **(b)** MoS<sub>2</sub>@C-H2, **(c)** MoS<sub>2</sub>@C-H4, **(d)** MoS<sub>2</sub>@C-H8, **(e)**MoS<sub>2</sub>@C-H12, **(f)** MoS<sub>2</sub>@C-H.

**Fig.S5** XRD patterns of **(a)** MoS<sub>2</sub>@C-L,**(b)** MoS<sub>2</sub>@C-H.

**Fig.S6** Raman spectra of MoS<sub>2</sub>@C.

**Fig.S7** TGA result of MoS<sub>2</sub>@C.

**Fig.S8** Rate capability of MoS<sub>2</sub>@C cycled at various rates from 0.1 to 5.0 A g<sup>-1</sup>.

**Fig.S9** MoS<sub>2</sub>@C-L8, MoS<sub>2</sub>@C-L12 and MoS<sub>2</sub>@C-L at a current density of **(a)** 0.2 Ag<sup>-1</sup>, **(b)** 1Ag<sup>-1</sup>.

**Fig.S10** MoS<sub>2</sub>@C-H8, MoS<sub>2</sub>@C-H12 and MoS<sub>2</sub>@C-H at a current density of **(a)** 0.2 Ag<sup>-1</sup>, **(b)** 1Ag<sup>-1</sup>.

**Fig.S11** EIS of **(a)** MoS<sub>2</sub>@C-L8, MoS<sub>2</sub>@C-L12 and MoS<sub>2</sub>@C-L,**(b)** MoS<sub>2</sub>@C-H8, MoS<sub>2</sub>@C-H12 and MoS<sub>2</sub>@C-H.

**Table S1**

	<b>MoS<sub>2</sub>@C-L</b>	<b>MoS<sub>2</sub>@C-H</b>
BET Surface Area(m <sup>2</sup> g <sup>-1</sup> )	64.3534	35.1899
Langmuir Surface Area(m <sup>2</sup> g <sup>-1</sup> )	65.7454	27.2338
Adsorption average pore size (nm <sup>2</sup> )	5.48244	5.19043
BJH Adsorption mean hole width(nm <sup>2</sup> )	14.7987	8.5994
BJH Desorption Mean Pore width(nm <sup>2</sup> )	5.9646	6.4407
Single point adsorption total pore volume of pores less than 40.4123 nm <sup>2</sup> width at P/P <sub>0</sub> = 0.950000000 (cm <sup>3</sup> g <sup>-1</sup> )	0.088203	0.045663
correlation coefficient	0.9999159	0.9998018

**Table S2**

	Rf( $\Omega$ )	Rct( $\Omega$ )
<b>MoS<sub>2</sub>@C</b>	449.5	72.3
<b>MoS<sub>2</sub>@C-L8</b>	1368	696
<b>MoS<sub>2</sub>@C-L12</b>	867.4	263.8
<b>MoS<sub>2</sub>@C-L</b>	937.5	342.4
<b>MoS<sub>2</sub>@C-H8</b>	538	137.1
<b>MoS<sub>2</sub>@C-H12</b>	1056	128.2
<b>MoS<sub>2</sub>@C-H</b>	1449	180

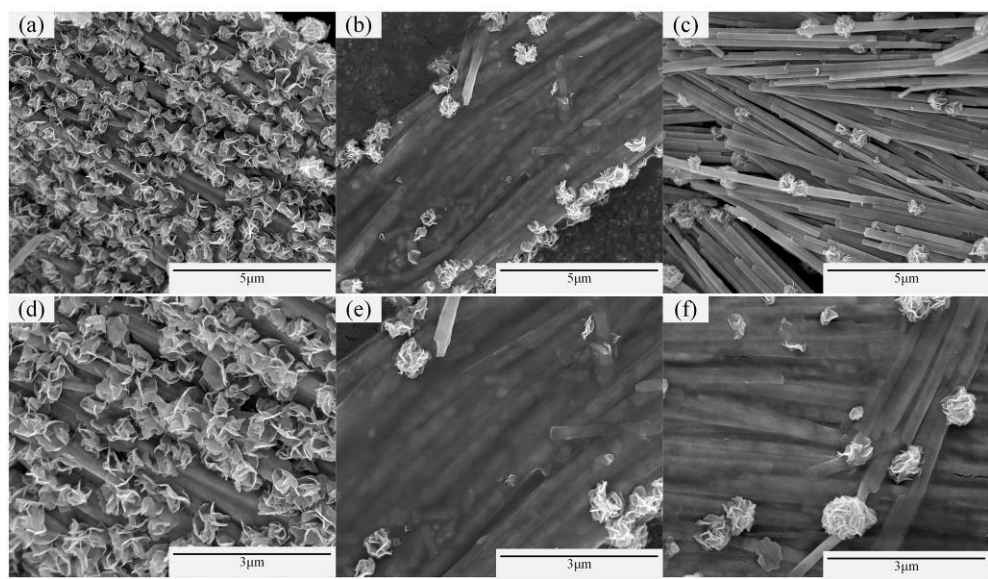


**Fig.S1**

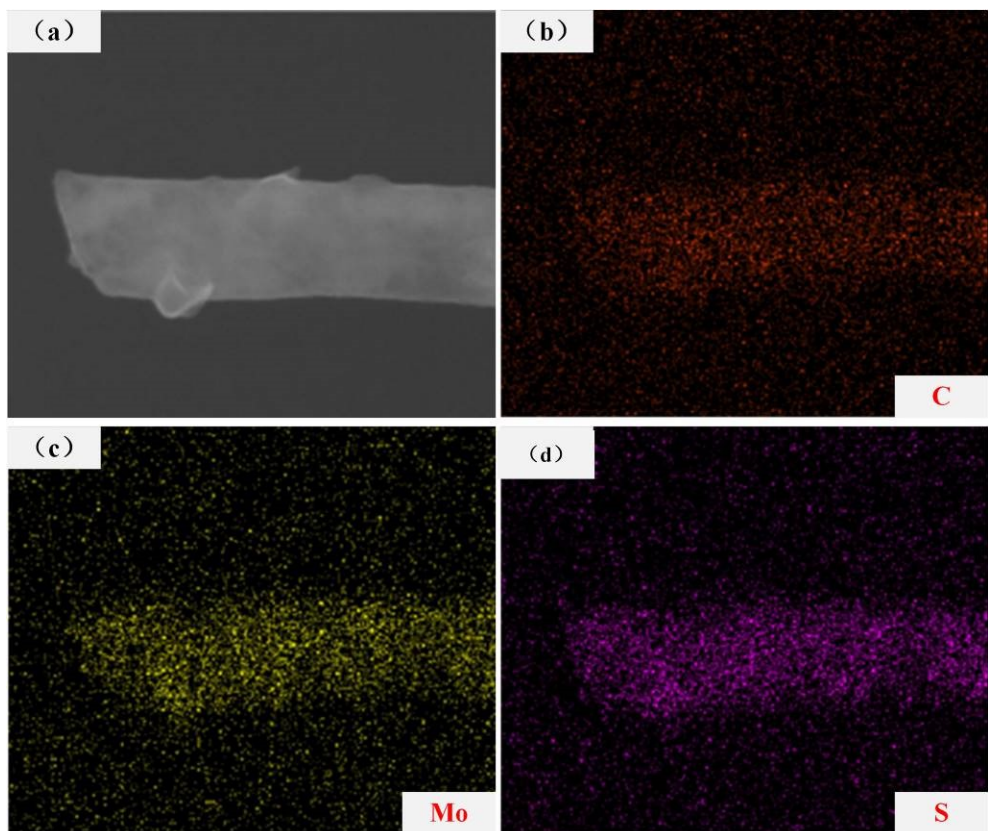


**Fig.S2**

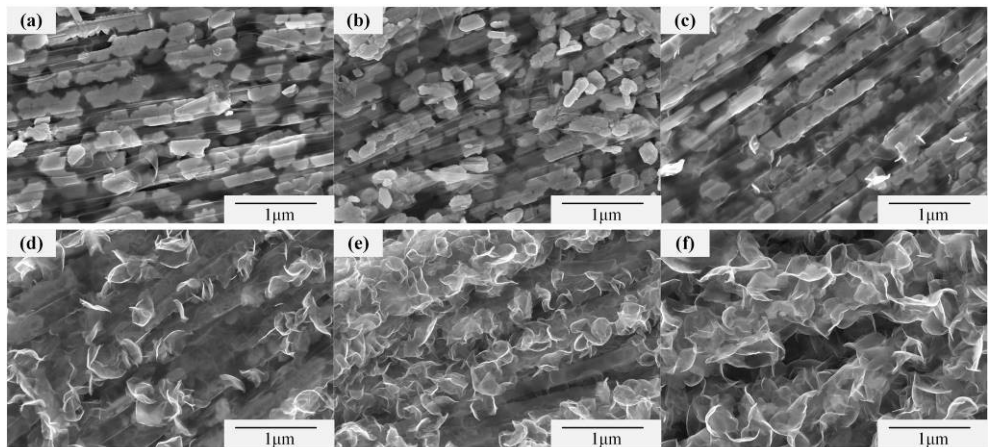


**Fig.S3**

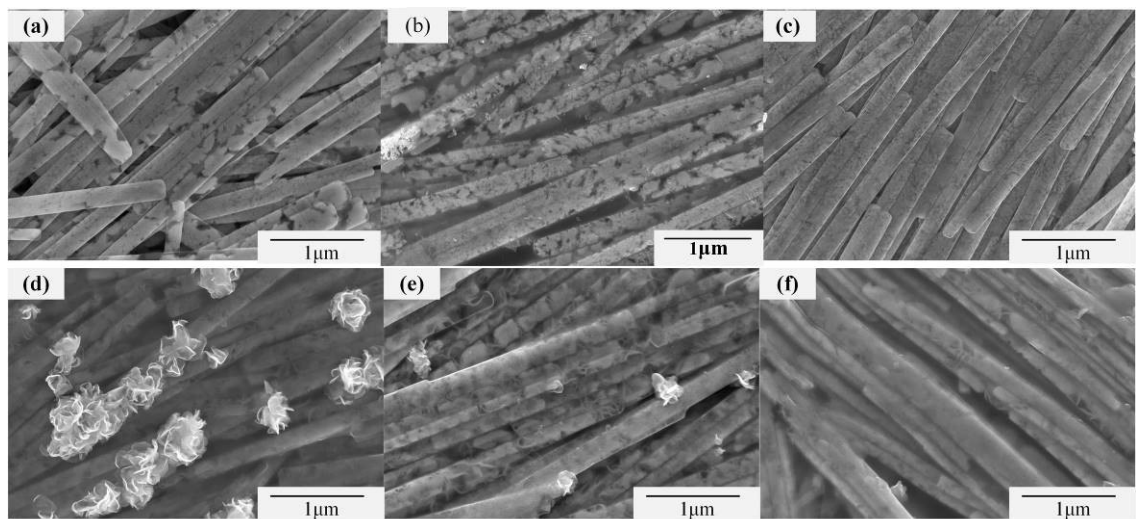


**Fig.S4**

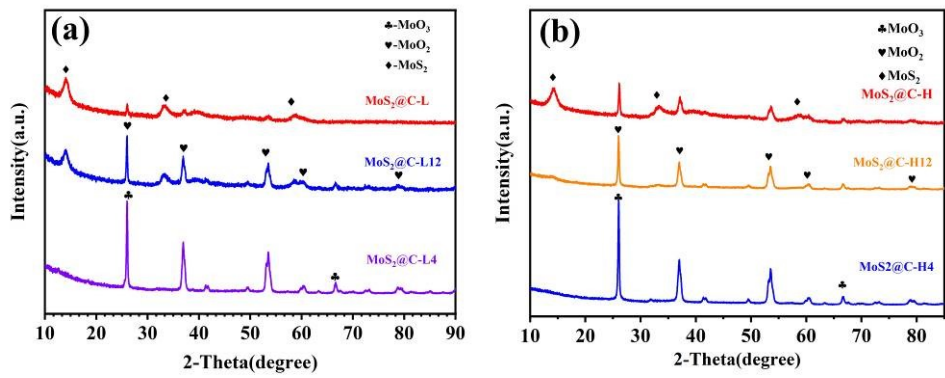


**Fig.S5**

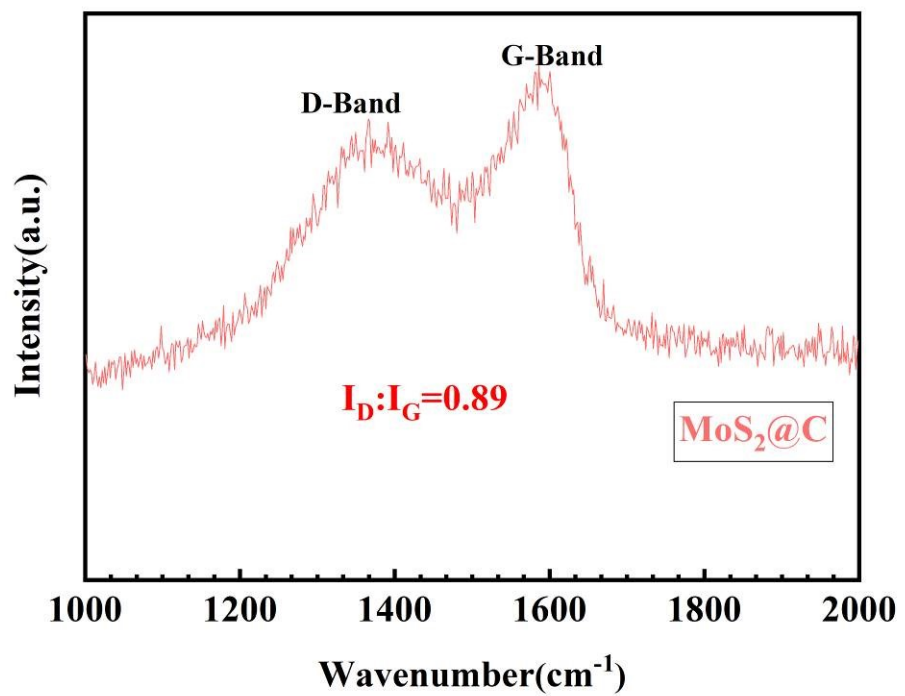
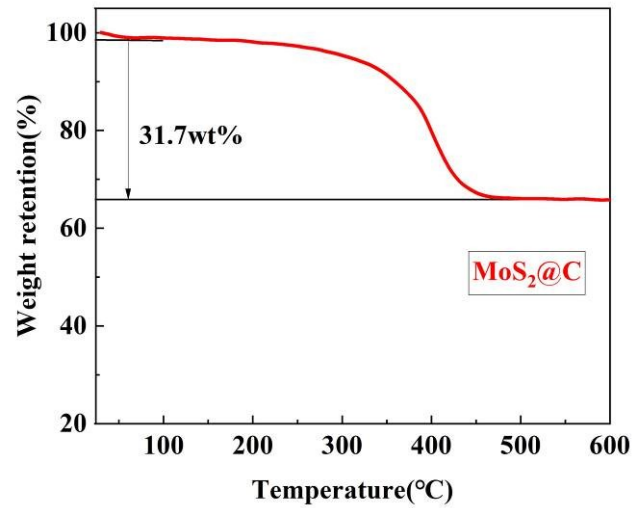


Fig.S6



**Fig.S7**

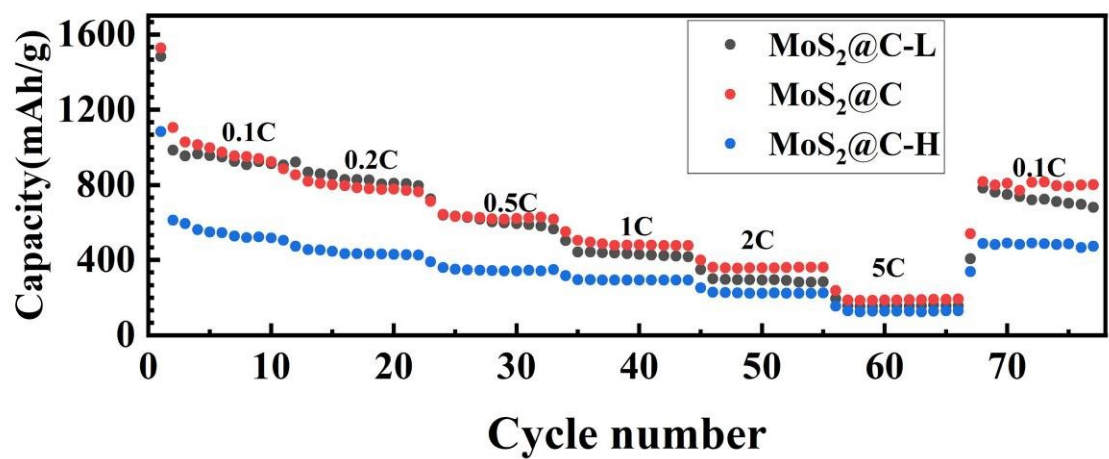


Fig.S8

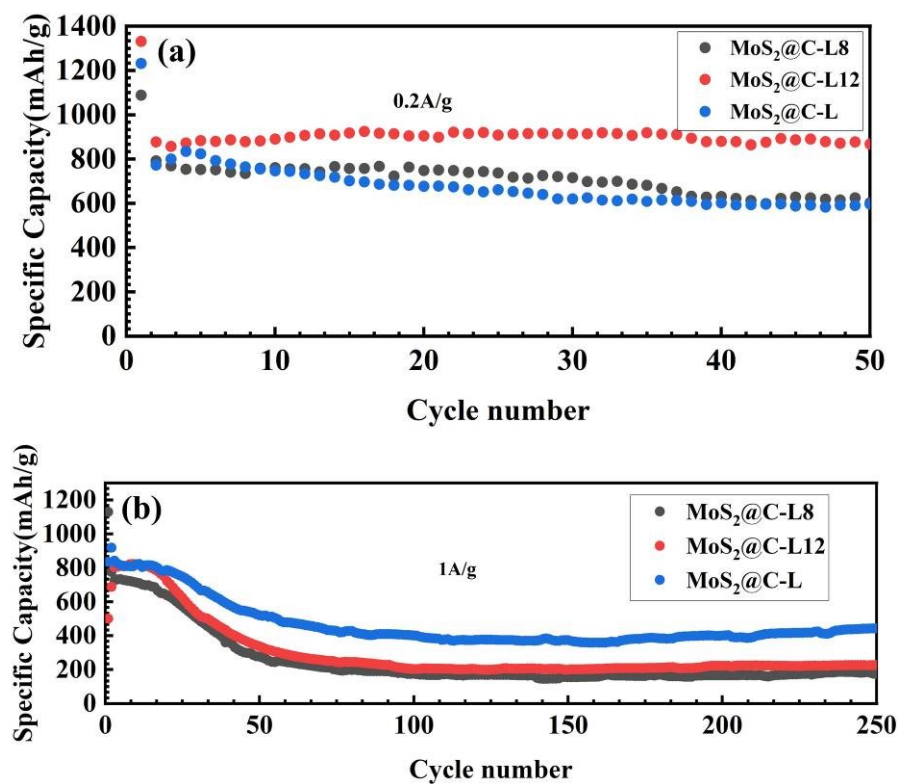


Fig.S9

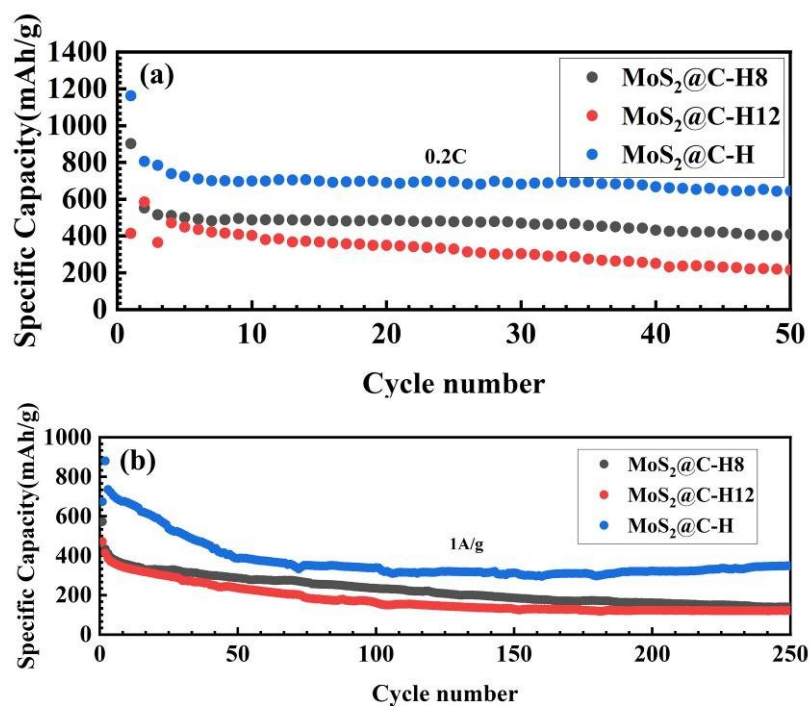
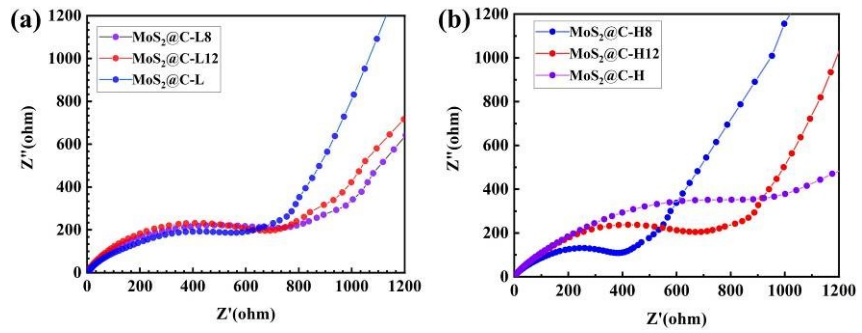


Fig.S10



**Fig.S11**